ISBN: 978-984-34-8313-3
www.iabse-bd.org

Parametric study on the lateral stiffness of carbon-fibre reinforced elastomeric isolators against cyclic loads

M.M. Riyadh
School of Engineering, University of British Columbia, Canada

F.H. Dezfuli
Bridge Engineer and Analyst, Parsons Corp., Canada

M.S. Alam
School of Engineering, University of British Columbia, Canada

ABSTRACT: Rubber bearings have a considerably low horizontal-to-vertical stiffness ratio which is well suited to mitigate the effects of seismic actions. The lateral performance of a base isolation system is predominantly a function of the horizontal stiffness in which the horizontal stiffness should be small enough to essentially decouple the structure from the ground motion. In this study, a parametric study is performed on Carbon-fibre Reinforced Elastomeric Isolators (C-FREI) with variable factors including number and thickness of rubber layers, thickness of the carbon-fibre reinforcement sheets, and loading area of the isolators. A 2^4 full factorial experiment is designed with four factors and two levels for each factor; the effectiveness of each factor was studied by examining the bearing's horizontal stiffness. It should be noted that the material models used for the 3D finite element modeling of the bearings in this study were verified against experimental results. From the analysis of variances, it is found out that the loading area has the most dominant effect, followed by thickness and number of rubber layers, whereas the thickness of carbon fibre-reinforcement sheets has negligible contribution in the horizontal stiffness of the C-FREIs.

1 INTRODUCTION

Earthquakes, as one of the most difficult to control phenomena due to their unpredictability, can have catastrophic consequences in human civilization. The effects of an earthquake can be reduced by a system of base isolation installed in both buildings and bridges. The idea of a base isolation system is to uncouple the structure by the addition of flexible pads between the substructure and superstructure. Elastomeric base isolators reduce the seismic load transmitted to the superstructure through a flexible damping mechanism. The isolation bearings contain considerable lateral flexibility which shifts the structure's fundamental period to evade resonance with the predominant frequency of the earthquake. Structures without seismic isolation is subjected to various range of cyclic loading which may lead to substantial story-drifts, whereas the structures with isolated bearings behave almost like a rigid body as large deformations are carried by the damping mechanism of the rubber bearings (Wang 2002).

This study focuses on the horizontal performance of Carbon-Fibre Reinforced Elastomeric Isolators (C-FREIs). Their lateral performance is explored by conducting numerical studies using material properties which were validated with experimental results. The effects of four input variables including number and thickness of rubber layers, thickness of carbon fibre-reinforcement sheets, and loading area of the bearings are probed for a two level, full factorial design. The effects are shown in terms of the C-FREI's horizontal stiffness, which is one of the operational characteristics of elastomeric bearings. The C-FREI's hysteresis behaviors are captured under two different shear strain levels. Analysis of variances (ANOVA) is implemented to interpret the results captured by FEM.

2 FIBRE-REINFORCED ELASTOMERIC ISOLATORS

Rubber bearings have to demonstrate a desired lateral flexibility, good energy dissipation, and sufficient vertical stiffness in order to be deemed functional. Steel reinforced elastomeric isolators (SREI) are the most common isolators in use but are limited to large and expensive structures as they are typically heavy and expensive. SREIs consists of rubber layers with steel shims as reinforcement between them. Fibre-reinforced

elastomeric isolators (FREIs) are a new type of elastomeric isolators that utilizes fibre as the reinforcement material rather than steel which provides FREIs several advantages such as, low manufacturing cost, light weight, and exceptional damping properties. Carbon fibres exhibit outstanding mechanical characteristics with a high tensile strength (2500-6000 MPa) and high elastic modulus (200-800 GPa) which makes them ideal candidates to be used as the reinforcement material in rubber bearings (Moon et al. 2002). Carbon Fibre-reinforced elastomeric isolators (C-FREI) are efficient in terms of production method and cost as they can be manufactured in the form of elongated rectangular strips followed by detailing and sizing through an automated process. Furthermore, unlike traditional SREIs, C-FREIs do not require a hot vulcanization process to establish a bond between the rubber and reinforcement layers (Kelly 1999). Several methods have been suggested to actuate the bonding process between the FRP and rubber layers. In one method, the bonding between carbon-fibre reinforced sheets and the rubber layers were initiated and propagated using rubber cement. This method saves energy as the cold vulcanization processes do not take as much energy and recourses as hot vulcanization process used in traditional base isolators (Toopchi-Nezhad et al. 2008). It was also suggested by Kelly to use microwave heating mechanism instead of applying heat and pressure to a mold. These methods of bonding proved to be successful and provided the bearings with adequate vertical rigidity and lateral flexibility.

The target horizontal stiffness in square isolators are often achieved by selecting a rubber material with a low shear modulus, i.e. rubber material having low stiffness. C-FREIs are investigated from different perspectives. For example,(Naghshineh et al. 2015) studied the comparison between C-FREIs and SREIs which concluded that at higher shear strain of smaller loading area bearings, there is a significant deviation in horizontal stiffness, and therefore a correction factor is suggested to be used with the traditional analytical equation. Another performance comparison between circular SREIs and C-FREIs has proven that fibre-reinforced elastomeric bearings have lower horizontal stiffness and considerably higher energy dissipation capacity than that of SREIs (Moon et al. 2002).A sensitivity analysis was performed to determine the effects of a range of parameters on the vertical and horizontal performance of C-FREIs. The study concluded that thickness of rubber layers has the most significant effect on the lateral performance of C-FREIs (Hedayati Dezfuli and Alam, 2014). Limited research has been conducted which primarily focus on the performance sensitivity of various factors on square C-FREIs, therefore a parametric study which focus on the effects of several factors on the horizontal stiffness will be performed in this study. Figure 1 shows the schematic view of the components of a C-FREI with end steel plates. As depicted from the figure, the main components of the C-FREIs are the rubber layers and C-FRP reinforcement sheets.

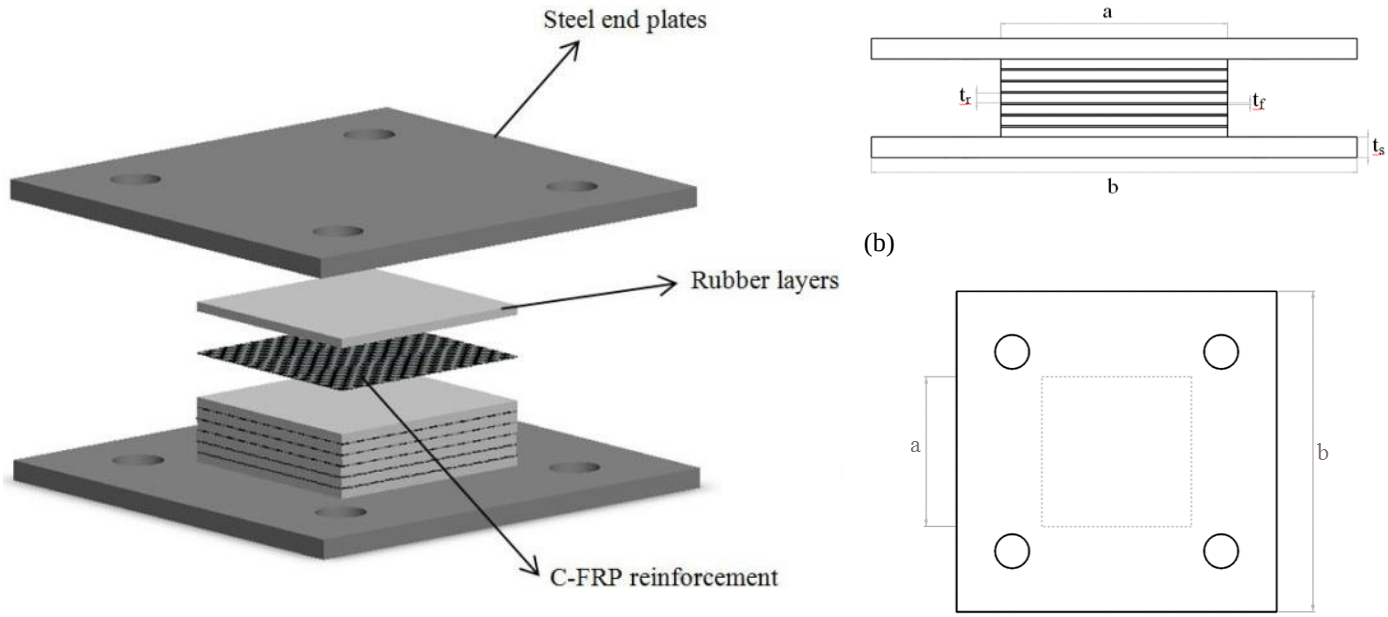

(a) (b) (c)

Figure 1. Schematic view of (a) C-FREI components (b) profile view (c) plan view.

where, a: length and width of the C-FREIs, b: length and width of the steel end plates,t_r: thickness of the rubber layers,t_f: thickness of the C-FRP reinforcement, t_s: thickness of the steel end plates.

3 NUMERICAL MODELLING AND VALIDATION

3.1 *Experimental Data*

A number of ¼ scale C-FREIs were manufactured using rubber layers having a durometer hardness rating of 55±5, C-FRP sheets between the rubber layers having a minimum tensile strength of 4413 MPa, and two supporting steel plates bonded to the top and bottom rubber layers. The bonding between the layers are achieved using a cold vulcanization process using rubber cement. The specimens are then subjected to constant vertical pressure of a specific magnitude without using a mold for 24 hours. One of the most common problems using carbon fibre sheets as the reinforcement material is the premature delamination which is minimized by applying adhesive layers at the sides of the specimens (Hedayati Dezfuliand Alam2014). Experiments had been conducted on only a limited number of samples and therefore, numerical modeling has been chosen to conduct this parametric study. In this regard, the experimental data of one of the manufactured samples were chosen to be compared with the finite element results to check the accuracy of the model. After validating the FE results, 16 C-FREIs are analyzed and modeled according to the 2^4 full factorial design.

3.2 *Finite Element Modeling*

The first step before proceeding with the numerical solution using finite element method is to configure the type of elements to be used. The elements chosen should comply with the material behavior of the model. In the next step, the material model is chosen followed by mesh discretization. Finally, the system is then analyzed and solved after applying boundary and loading conditions.

The modeling and analyzing of the C-FREIs were done in ANSYS (2019 R3). Element solid 186 with twenty nodes and three degrees of freedom at each node is selected for both steel end plates and rubber layers. Element shell 181 with four nodes and 6 degrees of freedom at each node is chosen for FRP sheets. The steel end plates are defined as an elastic isotropic material with a Young's modulus of 210 GPa and Poisson's ratio of 0.3 and the behavior of the FRP sheets are classified by orthotropic elasticity. The behavior of natural rubber under combined vertical pressure and cyclic lateral displacements is non-linear and complex and amongst several material models available in ANSYS, it is best described by the hyper-viscoelastic material model. Ogden second order hyperelastic material model is chosen to be simulating the hyperelastic behavior while the viscoplasticity is denoted by the Prony two term shear relaxation series which is time dependent. A perfect bonding is assumed between end steel plates, rubber and FRP layers, which allow no slip tolerance.

3.3 *Loading and Comparison*

The C-FREIs are subjected to a vertical pressure which is increased monotonically from zero to the design pressure (3MPa), in the first load step. Starting from the second load step, the bearings remain under the constant vertical pressure of 3MPa while cyclic lateral displacements are applied. Two levels of cyclic displacements (25%T_r, 50%T_r) are considered, where $T_r$the total thickness of the rubber layers given by is ($n_r t_r$). Three fully reversed sinusoidal cycles are applied at each shear strain level, having a time period of 1s and 2s, respectively. The loading variation for the vertical pressure and cyclic horizontal displacement against time are demonstrated in Figure 2. The bottom steel end plate is fixed in all directions while the load is applied to the top steel end plate.

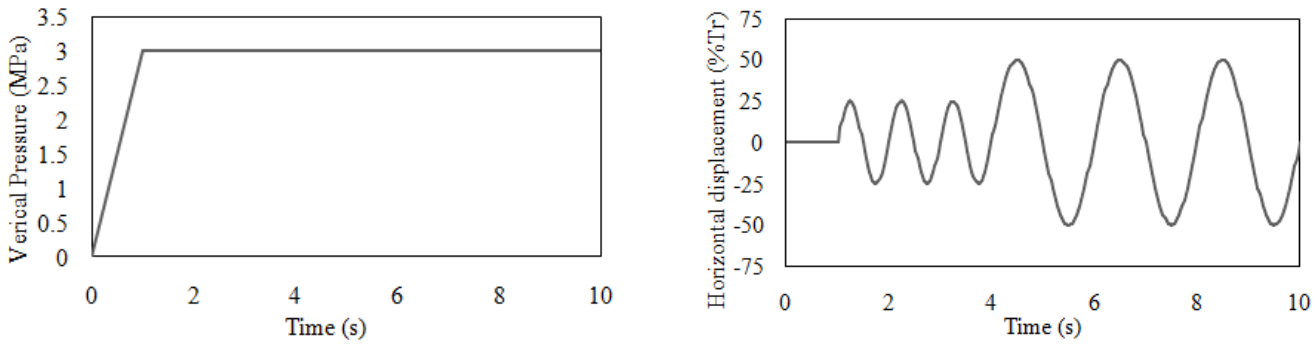

Figure 2. Vertical pressure and cyclic horizontal displacement used in this study.

The schematic of the C-FREI which is used for this validation of numerical results is shown in Figure 1. The C-FREI consist of $a = 70$mm, $b = 150$mm, $n_r = 7$, $t_r = 3$mm,$n_f = 6$, $t_s = 6.35$mm, and $t_f = 0.75$mm. Figure 3(a) shows the directional deformation in the horizontal direction of the C-FREI when subjected to

25% T_r shear strain. C-FRP sheets are modelled as thin shell elements and therefore cannot be visualized in the figure. The directional deformation is probed for the rubber layers excluding the steel end plates to better visualize the deformation pattern of the hyperelastic material. It is observed that the top rubber layer experiences the maximum lateral deformation when subjected to horizontal displacements while the bottom rubber layer experiences a higher deformation from the application of the vertical load.

The hysteresis behavior obtained from the simulation results are compared with the experiment hysteresis curve as shown in Figure 3(b). The dashed line displays the experimental results while the solid line displays the numerical solution results from the material models used in this study. As observed, the material model used for the simulation can accurately capture the nonlinear behavior of the bearing. The theoretical model is able to predict the horizontal stiffness of the experimental data with a deviation of less than 6%.

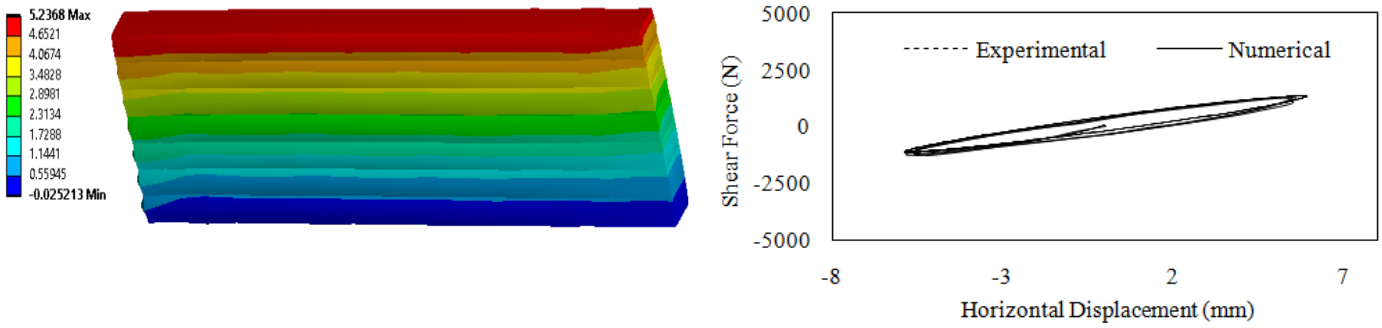

(a) (b)

Figure 3. (a). Directional deformation at 25% shear strain of the C-FREI used for validation. (b) Numerical material model validation with experiment.

4 PARAMETRIC STUDY

The performance of C-FREIs is affected by various physical and mechanical properties. A number of factors are described to express the performance of the rubber bearings. In this study, only the physical parameters which affect the effective horizontal stiffness will be taken into consideration. Amongst multiple physical parameters, the effective height of the rubber bearing is one of the most important factors which influences the performance of the rubber bearings. The effective height of the rubber bearingH_e, is a function of the thickness and number of rubber layers, as well as the number and thickness of C-FRP reinforcement sheets. The thickness of the steel end platest_s, is kept constant at 6.35mm and is not taken into consideration for calculating the effective height. It is because the end plates are considered to be rigid enough to not affect the lateral performance of the rubber bearings. Thus$H_e$can be represented by the following equation:

$$H_e = (n_r \mathrm{x} t_r) + (n_f \mathrm{x}\, t_f) \quad (1)$$

where n_r, t_r, n_f, $t_f$represents the number of rubber layers, thickness of rubber layers, number of C-FRP reinforcement layers, and the thickness of C-FRP reinforcement respectively. Number of C-FRP reinforcement layers n_f, is a function of the number of rubber layers denoted by:

$$n_f = n_r - 1 \quad (2)$$

As the number of C-FRP layers is a function of the rubber layers, it will not be considered as a separate factor in this parametric study. $H_e$is now a function of three factors and breaks down to:

$$H_e = (n_r \mathrm{x} t_r) + \left(t_f \mathrm{x} n_r\right) - t_f \quad (3)$$

The shape factor $S_F$is a characteristic of individual rubber layers which is defined by the ratio of loaded area to unloaded area. This parameter is calculated according to the following equation for square C-FREIs:

$$S_F = a^2/(4at_r) \quad (4)$$

The factors and levels to be varied for this parametric study is shown in Table 1. The length and width of the steel end plates b, are kept constant at 150mm.

Table 1. Parameters and their corresponding levels in the sensitivity analysis.

Factor	Symbol	Level	
		-	+
Number of rubber layers, n_r	A	7	10
Thickness of rubber layers, t_r	B	3 mm	6 mm
Thickness of FRP sheets, t_f	C	0.25 mm	0.75 mm
Loading area, (axa)	D	4,900 mm^2	22,500 mm^2

The operational characteristics to evaluate the full performance of C-FREIs are denoted by the vertical stiffness, horizontal stiffness, and equivalent viscous damping. Figure 4 shows a typical normalized mechanical model representing the hysteresis behavior of C-FREIs under cyclic load. The behavior of this model is described by the Ogden hyper-elastic material and Prony viscoelastic shear series. Hyper-viscoelastic material models can appropriately capture the behavior of high damping rubber bearings when subjected to combined vertical and shear deformations (Hedayati Dezfuli and Alam 2012).

The hysteresis curve provides a general idea of how the bearing behaves when subjected to combined vertical and cyclic shear loadings. Important characteristics such as effective horizontal stiffness (K_H) and equivalent viscous damping (β) are extracted from this model. The area inside the lateral force-deflection hysteresis curve denotes the energy dissipation capacity of the rubber bearings.

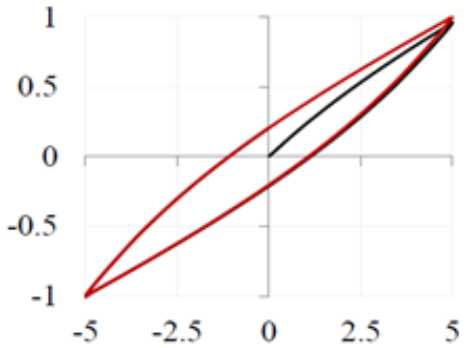

Figure 4. Cyclic loading response of C-FREIs using Ogden-Prony model (normalized lateral force vs. displacement) (Hedayati Dezfuliand Alam 2012).

The horizontal stiffness K_H, has been selected as the main response in this study. The lateral flexibility of the device is primarily determined from the effective horizontal stiffness which is one of the most important operational characteristics of an isolation system. It can be calculated by using equation (5) from the peak lateral forces (F_{max} , F_{min}) and the peak lateral displacements (γ_{max} , γ_{min}).

$$K_H = (F_{max} - F_{min})/(\gamma_{max} - \gamma_{\min}) \qquad (5)$$

With the purpose of consistency and providing a generalized tool, the factor level values are normalized and dimensionless by dividing each of them by their corresponding upper level (+) value. The normalized data are displayed in Table 2.

Table 2. Normalized parameters and their corresponding levels in the sensitivity analysis.

Factor	Symbol	Level	
		-	+
Number of rubber layers, n_r	$\hat{A}$	0.7	1.0
Thickness of rubber layers, t_r	$\hat{B}$	0.5	1.0
Thickness of FRP sheets, t_f	$\hat{C}$	0.3	1.0
Loading area, (axa)	$\hat{D}$	0.2	1.0

Having two levels defined for each factor in Tables 1 and 2, a total number of 16 runs are required to conduct a full factorial experiment for each shear strain level (2^4 full factorial experiment design), shown in Table 3. Considering two levels of strains, a total of 32 runs are generated for this experiment. Analyses of variances are carried out on the outputs to study the sensitivity of the bearing's performance under each factor.

Table 3. Runs conducted in 2^4 complete factorial design.

Run Order	A (n_r)	B (t_r)	C (t_f)	D (A_r)
1	+	-	-	-
2	-	+	+	+
3	+	+	+	+
4	+	-	+	+
5	+	-	+	-
6	-	+	-	-
7	-	+	-	+
8	-	-	-	-
9	+	+	-	+
10	+	+	+	-
11	-	-	+	+
12	-	-	-	+
13	+	-	-	+
14	-	+	+	-
15	-	-	+	-
16	+	+	-	-

5 RESULTS AND DISCUSSIONS

The horizontal stiffness of C-FREIs spanning the experimental space in finite element environment has been determined. In this regard, the FEM models produced in ANSYS are analyzed based on the model validation done in section 3. Different dimensions (width and height) of C-FREIs are produced which resulted from varying the thickness and number of rubber layers, carbon-fibre reinforcement sheet thickness, as well as the loading area. Their shear force versus displacement hysteresis loops are obtained from a total number of 16 combinations and the horizontal displacement is calculated according to equation (5).

Table 4. Output of the runs conducted in 2^4 full factorial design.

C-FREIs	$\widehat{A}$	$\widehat{B}$	$\widehat{C}$	$\widehat{D}$	$\hat{H}_e$	S_F	25%T_r		50%T_r	
							K_H (KN/mm)	$\hat{K}_H$	K_H (KN/mm)	$\hat{K}_H$
C1-1532	1.0	0.5	0.3	0.2	0.48	5.83	0.157	0.164	0.142	0.148
C2-7111	0.7	1.0	1.0	1.0	0.70	6.25	0.487	0.508	0.470	0.490
C3-1111	1.0	1.0	1.0	1.0	1.00	6.25	0.330	0.344	0.322	0.336
C4-1511	1.0	0.5	1.0	1.0	0.55	12.50	0.648	0.676	0.635	0.662
C5-1512	1.0	0.5	0.3	0.2	0.55	5.83	0.162	0.169	0.139	0.145
C6-7132	0.7	1.0	0.3	0.2	0.65	2.92	0.105	0.109	0.097	0.101
C7-7131	0.7	1.0	0.3	1.0	0.65	6.25	0.467	0.487	0.463	0.483
C8-7532	0.7	0.5	0.3	0.2	0.34	5.83	0.221	0.230	0.203	0.212
C9-1131	1.0	1.0	0.3	1.0	0.93	6.25	0.319	0.333	0.313	0.326
C10-1112	1.0	1.0	1.0	0.2	1.00	2.92	0.075	0.078	0.069	0.072
C11-7511	0.7	0.5	1.0	1.0	0.38	12.50	0.956	0.997	0.905	0.944
C12-7531	0.7	0.5	0.3	1.0	0.34	12.50	0.959	1.000	0.914	0.953
C13-1531	1.0	0.5	0.3	1.0	0.48	12.50	0.671	0.700	0.619	0.645
C14-7112	0.70	1.00	1.00	0.22	0.70	2.92	0.110	0.115	0.101	0.105
C15-7512	0.70	0.50	1.00	0.22	0.38	5.83	0.221	0.230	0.203	0.212
C16-1132	1.00	1.00	0.33	0.22	0.93	2.92	0.070	0.073	0.065	0.068

Their naming, geometrical properties, and effective horizontal stiffness as response output are presented in Table 4. The specimens are numbered from C1 to C16 depending on their run order, which is the first designation of their naming notation. Each digit in the second designation represents their normalized modification characteristic of the four factors in the order A-D. A value of 1 represents a high level modification while a low level modification is denoted by the digit after the decimal. For example, C-FREI C1-1532 has 10 number of rubber layers [n_r, high (+)], 3mm as the thickness of rubber layers [t_r, low (-)], 0.25mm thickness of C-FRP reinforcement sheets [t_f, low (-)], and loading area of 4,900mm^2[axa, low(-)].

H_e of the rubber bearings are calculated using equation (3) and are normalized by dividing each bearing's effective height by the maximum effective height. The $S_F$values of the combination specimens are determined from equation (4). The output horizontal stiffness response is normalized by dividing each value with the highest response output of horizontal stiffness from both levels of shear strain for ease of comparison.

5.1 *Analysis of Variance*

Only the main factor effects were examined in order to get the half probability effect plot shown in Figure 5. For a 95% confidence interval, the main factors A (number of rubber layers), B (thickness of rubber layers), and D (loading area) were found to have significant effects on the horizontal stiffness. The effect of factor C (thickness of the C-FRP reinforcement) is found to be insignificant on the output response.

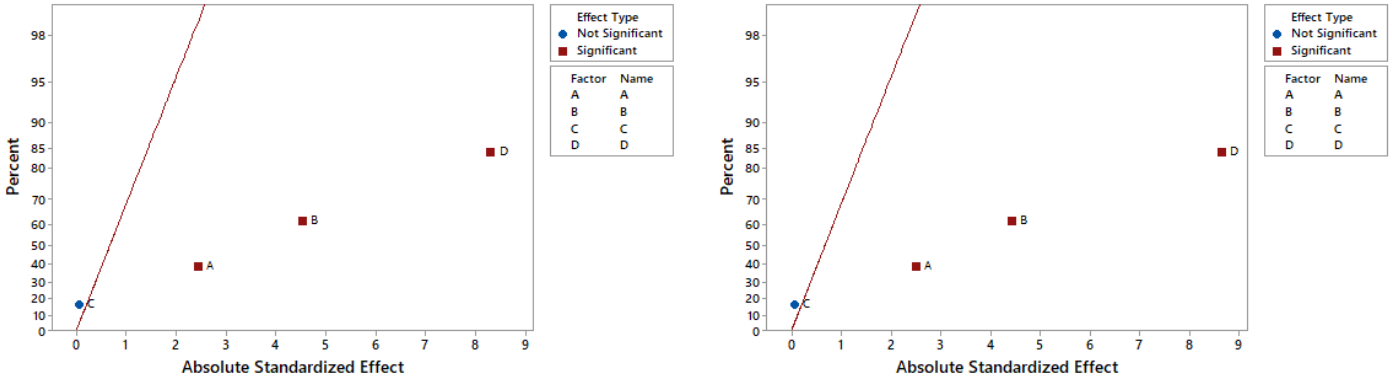

(a) (b)

Figure 5. Half normal probability plot for absolute standardized factor effect at (a) 25%T_r and (b) 50%T_r

Factors having larger distance from the slope has a greater effect on the output horizontal stiffness. It is also observed from the output test results that the C-FREIs possess a slightly lower horizontal stiffness value for higher shear strain level. This is due to displacement-dependency of rubber material properties which causes the horizontal stiffness to decrease at larger shear strain levels. This happens as rubber material loses its stiffness more due to getting more in the inelastic range.

As the results obtained are from numerical simulations, no replicates or error degree of freedom is accessible to conduct the ANOVA. Hence, the higher order interaction terms (third and fourth order) were used to introduce an error degree of freedom into the model. The P-values of the significant factors (A,B, and D) were found to be much smaller than the α value of 0.05, so the assumptions made from Figure 5 did not change. Figure 6 demonstrates the surface plots of the mean normalized response output and a pair of factors for higher level of lateral displacement. It is observed that factor D contributes towards a positive correlation and factors A and B contributes towards a negative correlation towards the output response. From Figures 5 and 6, it can be concluded that factor D has the highest effect on the horizontal stiffness, followed by factors B and A.

5.2 *Effective Height and Shape Factor on the Horizontal Stiffness of C-FREIs*

Figure 7 shows the normalized horizontal stiffness by the normalized effective heights.H_e varies in the range of 22.5 - 66.75mm by varying the factors A, B, and C.

The average response of factor C was found to be insignificant according to section 5.1 and hence, only the combinations of C-FREIs having lower level values of C are used for comparisons in effective height. It can be seen that for both levels of loading area, the horizontal stiffness reduces with increasing the effective height, improving the bearing's performance in the lateral direction. The rate of decrease in horizontal stiffness with increasing height is more pronounced for higher loading area. The horizontal stiffness reduces with increasing the shear strain amplitude. This reduction becomes less noticeable at larger effective heights.

The shape factor is a function of the loading area and the thickness of the rubber layers. Having two levels of loading area and thickness of rubber layers leads to two different values of S_F under a single loading area. Figure 8 demonstrates the plot of normalized horizontal stiffness by the shape factors of the combinations of C-FREIs having higher values of C-FRP thickness.

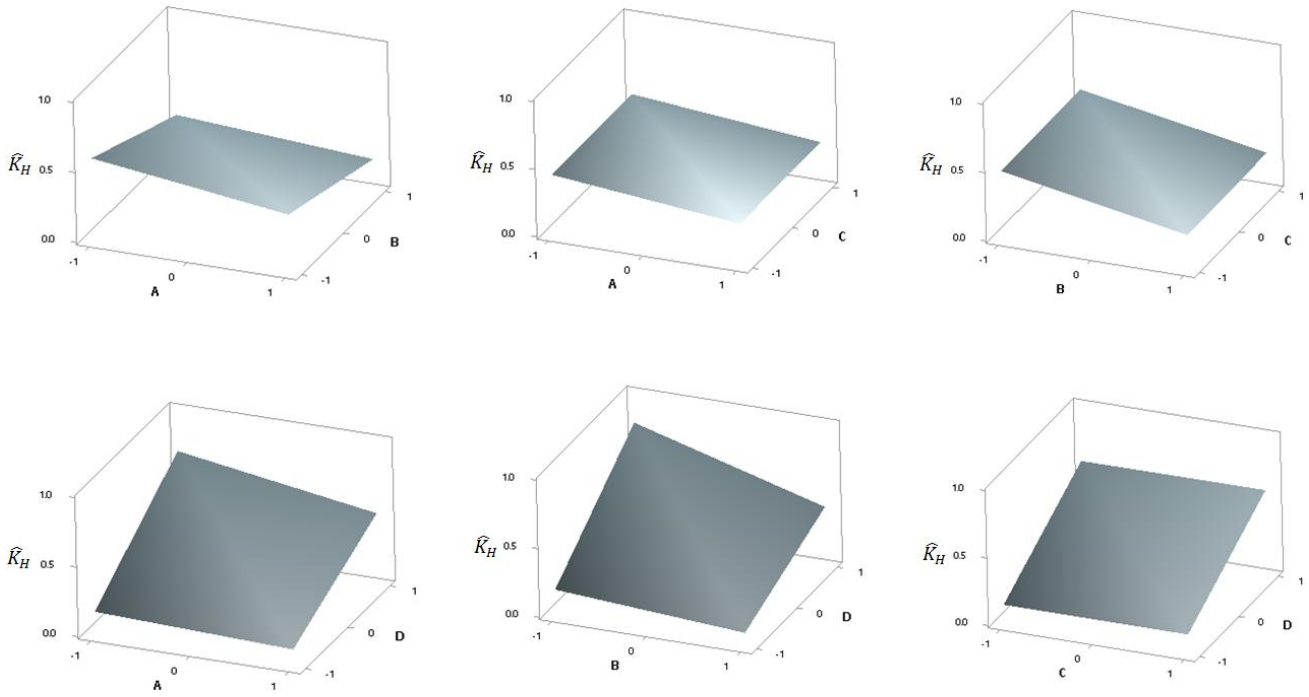

Figure 6. Surface effect plots for a pair of factors at 50% shear strain.

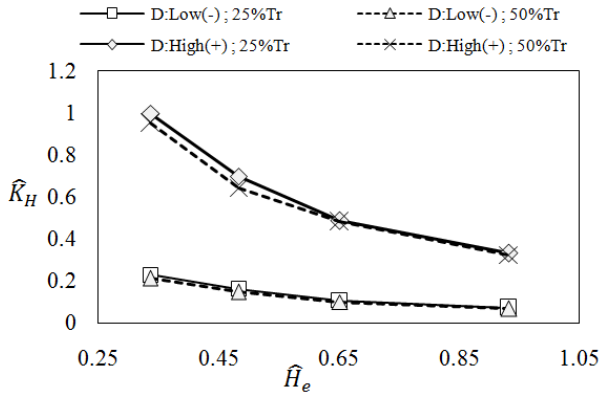

Figure 7. Comparison of horizontal stiffness by effective height.

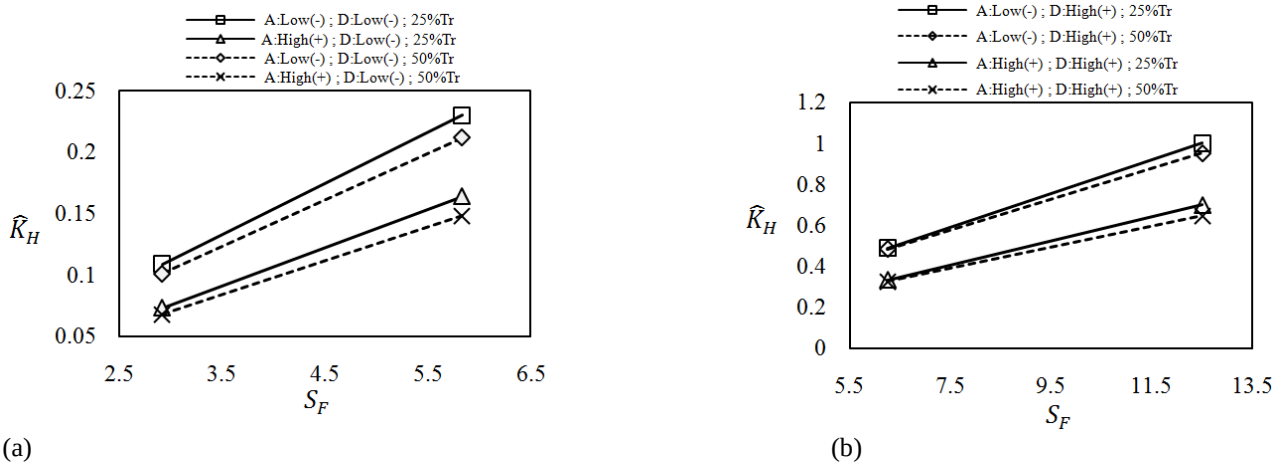

(a) (b)

Figure 8. Comparison of horizontal stiffness by shape factor (a) for lower level of loading area (b) for higher level of loading area.

According to the plots, increasing the shape factor causes an elevation to the horizontal stiffness for both loading areas. As consistent with all the results, the horizontal stiffness reduces for higher lateral displacement and this reduction becomes more noticeable at larger shape factor values. Moreover, combinations of C-FREIs possessing equal magnitudes of primary shape factor displays a greater value of horizontal stiffness having lower number of rubber layers.

6 CONCLUSIONS

The main aim of this study is to investigate the sensitivity of several factors on the output lateral stiffness of rubber bearings by changing the factor levels from a low value to a high value. The horizontal stiffness for 16 combinations under cyclic loads was evaluated using finite element method. It should be noted that the material model used in this approach (i.e. FEM) was validated against experimental results. The analyses were conducted on square C-FREIs having different dimensions: two different levels of loading area, number and thickness of the rubber layers, and thickness of the C-FRP reinforcement. From the results obtained, the following conclusions have been drawn:

- The horizontal stiffness of C-FREIs reduces for higher level of shear strain for all considered factors. Rubber material goes more towards the inelastic range at higher shear strains which causes the stiffness to reduce due to the displacement dependency characteristic of rubber material.
- Changes in effective height of C-FREIs results from varying the number and thickness of the rubber layers, as well as the C-FRP reinforcement. The horizontal stiffness reduces with an increase in the effective height. This reduction is mostly dependent on the total thickness of rubber layers as the rubber material is mainly responsible for the horizontal flexibility of rubber bearings. The drop in horizontal stiffness occurs at a greater rate for C-FREIs having a larger loading area. It is also observed that the drop in stiffness values by increasing the shear strain is higher for C-FREIs having greater effective height.
- A greater shape factor (defined as the ratio of the loaded area to the side load free area of each rubber layer) results in the bearings with a larger horizontal stiffness. The strain dependency characteristic of the rubber material in C-FREIs for higher shear strain also cause the horizontal stiffness to drop more rapidly at higher shape factors. C-FREIs possessing equal shape factors have a greater horizontal stiffness for lower number of rubber layers.
- According to the analysis of variances, the loading area of the C-FREIs has the greatest influence on the horizontal stiffness with a positive correlation. A greater loading area leads to a greater horizontal stiffness degrading the bearings' flexibility in the lateral direction. Increase in both the number and thickness of the rubber layers lowers the horizontal stiffness of the C-FREIs, enabling the bearings to mitigate large lateral displacements. It should also be noted that the thickness of the rubber layers has a greater effect on the horizontal stiffness than the number of rubber layers. The thickness of the C-FRP reinforcement was found to have negligible effect in the horizontal stiffness of C-FREIs with a confidence interval of 95%. This can be justified due to the fact that carbon-fibre sheets possess almost no flexural rigidity and have very little contribution towards the horizontal stiffness.

REFERENCES

Hedayati Dezfuli, F, & Alam, M. S. (2012). *Material Modeling of High Damping Rubber in Finite Element Method*.

Hedayati Dezfuli, F., & Shahria Alam, M. (2014). Performance of carbon fiber-reinforced elastomeric isolators manufactured in a simplified process: Experimental investigations. *Structural Control and Health Monitoring*, 21(11), 1347–1359.

Hedayati Dezfuli, Farshad, & Alam, M. S. (2014). Sensitivity analysis of carbon fiber-reinforced elastomeric isolators based on experimental tests and finite element simulations. *Bulletin of Earthquake Engineering*, 12(2), 1025–1043.

Karimzadeh Naghshineh, A., Akyuz, U., & Caner, A. (2015). Lateral response comparison of unbonded elastomeric bearings reinforced with carbon fiber mesh and steel. *Shock and Vibration*.

Kelly, J. M. (1999). Analysis of Fiber-Reinforced Elastomeric Isolators. In *JSEE: Fall* (Vol. 2).

Moon, B.-Y., Kang, G.-J., Kang, B.-S., & Kelly, J. M. (2002). *Design and manufacturing of fiber reinforced elastomeric isolator for seismic isolation*.

Toopchi-Nezhad, H., Tait, M. J., & Drysdale, R. G. (2008). Testing and modeling of square carbon fiber-reinforced elastomeric seismic isolators. *Structural Control and Health Monitoring*, 15(6), 876–900.

Wang, Y.-P. (2014). *Fundamentals of Seismic Base Isolation*.